

ANN AND HYBRID MODELLING OF ECCENTRICALLY PATCH LOADED STEEL I-GIRDERS

Biljana Šćepanović¹, Snežana Rutešić¹, Olga Mijušković¹,
Luisa María Gil-Martín², Enrique Hernández-Montes²

¹University of Montenegro, Podgorica, Montenegro

²University of Granada, Granada, Spain

Abstract. Majority of eccentrically patch loaded girders collapse at lower load level than their geometrical equivalents loaded in the web plane, due to different collapse mechanism. However, some eccentrically patch loaded girders, even with significant load eccentricity, behave as if loaded in the web plane, having the same collapse mode and ultimate load as in the case of centric load. Hence, the ultimate strength of eccentrically patch loaded steel I-girders should be found out in two phases: firstly, girder collapse mode should be estimated; secondly, depending on expected collapse mode, ultimate load should be calculated appropriately. Both tasks are demanding, with plenty of mutually dependent influential parameters. Artificial neural network (ANN) modelling, being suitable for multi-parameter analysis, is quite convenient method for studying eccentrically patch loaded steel I-girders in both mentioned tasks, as confirmed through the examples elaborated in the paper. Not only that it is valuable on its own, as a standalone technique, but also in combination with and as support to other methods (hybrid modelling).

In comparison of five procedures for ultimate load determination (empirical expression, mechanical model, two versions of refined mechanical model, one of them by ANN, and standalone ANN forecast model), ANN modelling, providing high quality results, qualified in top-two procedures for ultimate load, regardless of collapse mode type. It is also proved that certain shortages of mechanical model may be overcome by its coupling with ANN modelling. Such hybrid modelling provided remarkably more accurate results than original mechanical model.

Study confirmed need of revision of mechanical model. As the first step, new, more demanding constraints of mechanical model validity are proposed in this paper.

Key words: Eccentric patch load, Collapse mode, Ultimate load, Artificial neural network, Hybrid modelling

Received: January 10, 2024 / Accepted March 15, 2024

Corresponding author: Biljana Šćepanović

University of Montenegro, Faculty of Civ. Eng. Bul. Džordža Vašingtona bb, 81000 Podgorica, Montenegro

E-mail: biljanas@ucg.ac.me, biljajs38@gmail.com

1. INTRODUCTION

The term “patch load” designates the load acting over a small area or length of a structural element, as a concentrated or locally distributed load, Fig. 1. A typical situation in structural engineering practice is when compressive patch load affects the flange of I-profile so that the web is locally pressed in the zone under the loading. Local compression might provoke local instability that may result in element carrying capacity loss and, consequently, collapse of the whole structure. Patch load examples are numerous and present in different types and segments of structures, such as crane girders loaded by crane wheels, bridge girders during erection by launching, rafters supporting secondary girders, column-beam joints, ship structures subjected to truck wheel or steel coil, etc. [1-3].

A comprehensive research work has been done worldwide, tackling different aspects of patch loaded steel I-girders [4,5]. The main research topic is the ideal case of patch load acting in the web plane, i.e. centric patch load, Fig. 1a. Numerous experimental studies provide solid amount of data as a base for further statistical, numerical (primarily by finite element method (FEM)) and analytical modelling, enabling proposals of different plastic collapse mechanisms, their mathematical formulations and adjoining expressions for ultimate load calculation. Increase in web (buckling) stability and girder resistance to patch load may be achieved by: (a) increase in web thickness; (b) longitudinal (web) stiffeners [6]; (c) transverse stiffeners [7]; (d) simultaneous transversal and longitudinal stiffening [8]; (e) delta stiffeners, i.e. triangular cell loaded flange [9,10]; (f) use of corrugated instead of flat web plates [11,12]. Not all these measures are fully efficient in case of load that changes its position (e.g. cranes, bridges, ships, etc.). Furthermore, production of such girders may be cost/time demanding. Hence, the rationalisation of patch loaded I-girders with unstiffened, flat web plate is still in focus of research. Additionally, investigation attention in this domain is still devoted to specific influential parameters and circumstances, such as: initial conditions (geometry imperfections and residual stresses) [13,14]; patch load length [14,15]; interaction of patch loading with bending and/or shear [16], etc. In line with needs of environmental protection and cost-effectiveness, hybrid steel I-girders (with different mechanical properties of flange/web steel) [17], as well as options of substitution for mild steel (aluminium [18], stainless steel [19], high-strength steel I-girders [20]) or its upgrade by cladding (I-girders having mild steel web, clad by titanium [21] or stainless steel [22]) have been studied recently. A girder behaviour under patch loading at elevated temperatures or in fire conditions is analysed [23]. A piece of research findings concerning centric patch loading is implemented in European design standards, Eurocodes – EN1993-1-5 [24]. However, review and further adjustments of standards are needed, so to avoid too low underestimation of ultimate load, as well as to cover more diverse cases regarding girder geometry and load arrangement.

In the engineering reality, a certain eccentricity of patch load relative to the web plane is unavoidable, i.e. eccentric patch load is more realistic case, Fig. 1b. This case is among issues which are not currently incorporated in Eurocodes, with the appropriate calculation procedure. In some circumstances, the load eccentricity may be treated as an imperfection that will not cause significant change in girder’s behaviour and carrying capacity compared to the centric load case. However, in other situations the load eccentricity should not be neglected, since it may be the reason for dangerous decrease in ultimate load (even up to 75%), as a result of girder’s behaviour being completely different from the one of centrally loaded girder.

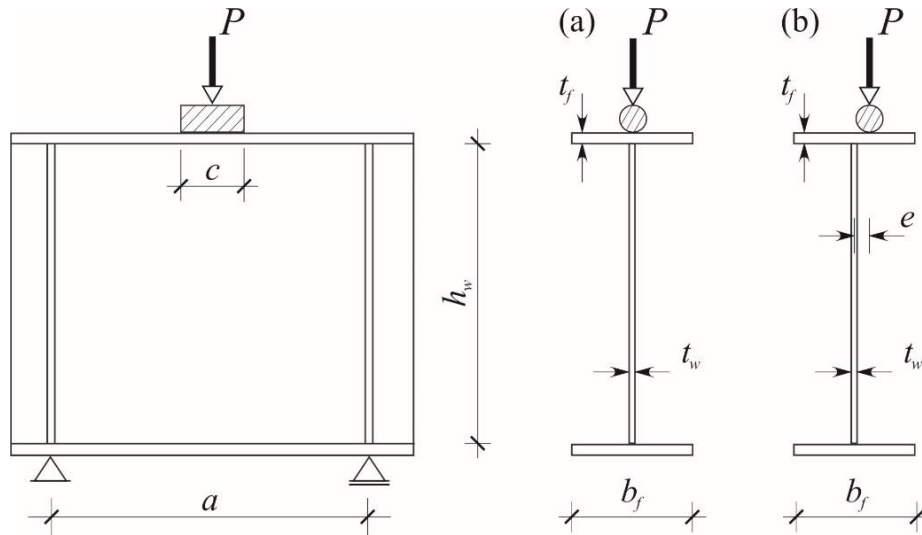


Fig. 1 Patch loaded steel I-girder: (a) centric patch load; (b) eccentric patch load [25]

Compared with the case of centric patch load, rather modest amount of research has been devoted to the case of eccentric patch load. While over 40 experimental researches (with more than 800 tested samples) dealt with centrally patch loaded I-girders, influence of load eccentricity was analysed in only eight experimental studies (with less than 200 tested samples). Majority of tests (135 specimens) were done at the University of Montenegro, in three series of experiments, in: 1998, reported by Lučić [26]; 2001, reported by Lučić and Šćepanović [27]; and 2007, reported by Šćepanović et al. [28]. The latest testing, with only four tested girders, was done at the University of Navarra, upon the initiative of the University of Granada, in 2009, reported by Gil-Martín et al. [29]. Experimental work was followed by non-linear finite element method (FEM) modelling [28,29]. While over 30 mathematical expressions (mostly based on collapse mechanism) for centric ultimate load might be found in scientific literature and design norms, only one mathematical/mechanical model for eccentric ultimate load calculation, based on the plastic collapse mechanism, is published by Graciano and Uribe-Henaó [30]. Prior to the development of this mathematical/mechanical model, a few empirical expressions for eccentric ultimate load have been proposed, last modifications by Šćepanović et al. [28] and Gil-Martín et al. [29]. Design norms still do not encompass eccentric patch load. Arabzadeh and Varmazyari [9] analysed influence of delta stiffeners in eccentrically patch loaded girders, by means of FEM modelling. Inaam and Upadhyay [11], as well as Maiorana, Poh'sié and Emechebe [12] touched on an issue of eccentric patch load in girders with corrugated web, in their FEM based analyses.

Experimental research demonstrated that majority of eccentrically patch loaded girders collapse at lower load level than their geometrical equivalents loaded in the web plane. Lower ultimate load is a consequence of different girder's behaviour, i.e. different collapse mechanism or collapse mode, in case of eccentric load (flange warping/twisting, followed by web bending) compared with the case of centric load (web buckling, followed by flange "sinking"), Fig. 2.

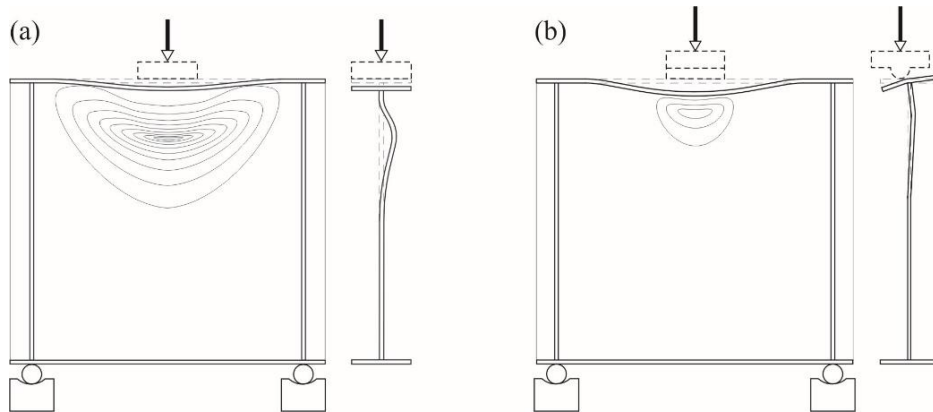


Fig. 2 Collapse modes typical for centric and eccentric patch load:
(a) centric collapse mode; (b) eccentric collapse mode [25]

However, some eccentrically patch loaded girders, even with significant load eccentricity, behave as if loaded in the web plane, having the same collapse mode and ultimate load as in the case of centric load. Hence, the ultimate strength of eccentrically patch loaded steel I-girders should be found out in two steps: at first, girder collapse mode should be estimated; secondly, depending on expected collapse mode, ultimate load should be determined appropriately. Obviously, it is rather complicated task to formulate unique mechanical model (i.e. collapse mechanism and ultimate load expression based on it) that may be applied to all eccentrically patch loaded girders.

Numerous parameters and their combinations determine behaviour, i.e. collapse mode and ultimate load of eccentrically patch loaded girders. The most prominent one is the load eccentricity, e , Fig. 1b. Girder dimensions, Fig. 1, primarily plate thicknesses, t_w and t_f , as well as dimensionless geometry parameters, such as t_f/t_w , h_w/t_w , etc. are also of a great significance. A change of only one girder dimension results in the variation of several influential parameters, what makes the analysis rather complex.

Various artificial intelligence (AI) methods and techniques are highly suitable for multi-parameter analysis, particularly for solving compound stochastic problems, characterised with plenty of uncertainties and inter-dependencies. Artificial neural networks (ANN), machine learning (ML), deep learning (DL), etc. are nowadays fairly present in different areas of structural engineering, with high potential to complement, alternate or even replace traditionally used empirical modelling, based on statistics methods, and FEM based numerical modelling, as summarised in comprehensive reviews of Salehi and Burgueño [31], Sun et al. [32], Wang et al. [33], Tapeh and Naser [34]. Widening field and growing number of examples of successful ANN applying in design, construction, protection, monitoring and maintenance of diverse structures, such as reported by Chojaczyk et al. [35], Markovic et al. [36], Zarezadeh et al. [37], include the topic of patch loading, too.

ANN modelling/forecasting, as a sophisticated AI calculation and modelling method, is quite convenient approach for studying centrally patch loaded I-girders, as presented by Kurtoglu et al. [18], Mai et al. [38], Kumar et al. [39]. In case of eccentric patch load, with all its complexity and intricacy, ANN modelling is even more welcome and valuable,

as demonstrated by Šćepanović et al. [25]. However, this technique has not been used to its full potential, which is evident in both phases of eccentrically patch loaded steel I-girders analysis: collapse mode estimation and ultimate load determination.

ANN modelling may be successfully used on its own, but also as an advantageous tool coupled with other methods (i.e. hybrid modelling), e.g. with the only one existing mechanical model of collapse mechanism or with some of only few existing empirical expressions for ultimate load calculation. Benefits of ANN modelling, as well as hybrid modelling are elaborated in the paper, through the examples.

2. COLLAPSE MODES OF ECCENTRICALLY PATCH LOADED STEEL I-GIRDERS

Eccentrically patch loaded steel I-girders mostly lose carrying capacity due to local elastic-plastic bending, with emphasised flange torsion and almost undeformed web, as in Fig. 3, but not necessarily. As already mentioned, under certain circumstances, eccentrically loaded girders may lose carrying capacity the same way as if there is no load eccentricity. Three different types of collapse mode, each with several variants, are observed in experimentally tested eccentrically patch loaded steel I-girders: eccentric (E, Fig. 3), centric (C, Fig. 4) and mixed (M, Fig. 5) collapse mode.

Flange torsion, web deformation, position and shape of yielding lines (primarily one in web, but also one in flange), as well as their development level, in case of eccentric collapse mode, vary, depending on girder geometry and load eccentricity, as displayed in Fig. 3.

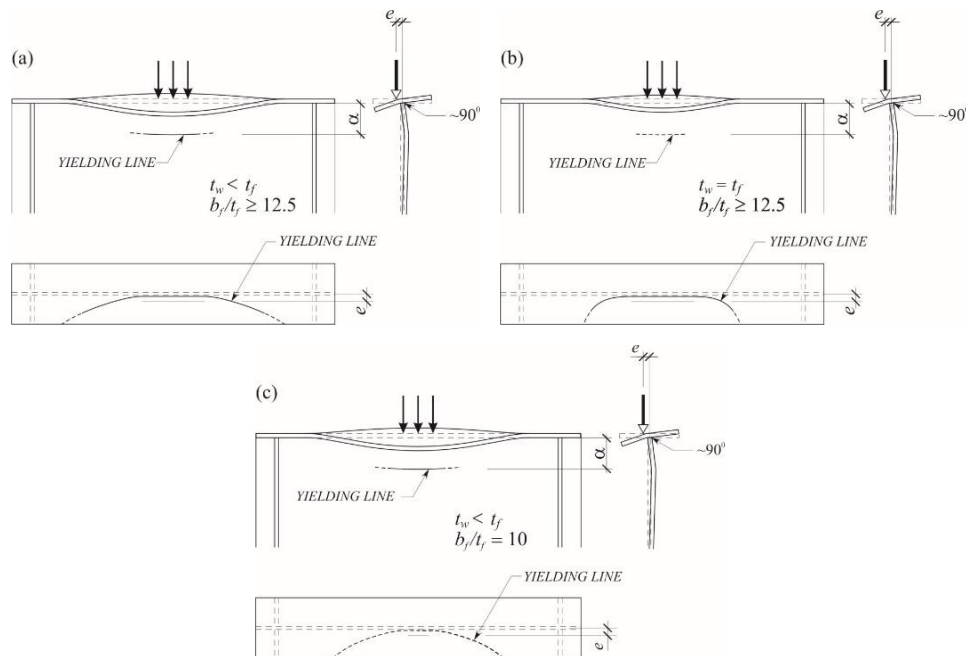


Fig. 3 Eccentric collapse mode of eccentrically patch loaded I-girders (E) – variants, depending on girder geometry:

(a) $t_w < t_f$ & $b_f/t_f \geq 12.5$; (b) $t_w = t_f$ & $b_f/t_f \geq 12.5$; (c) $b_f/t_f = 10$ (thick flange)

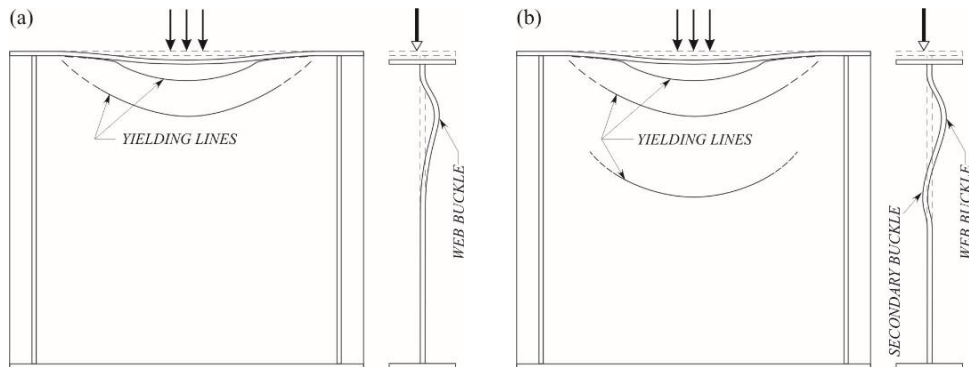


Fig. 4 Centric collapse mode of eccentrically patch loaded I-girders (C) – variants:
 (a) with two yielding lines (and one buckle) in web;
 (b) with three yielding lines (and two buckles) in web

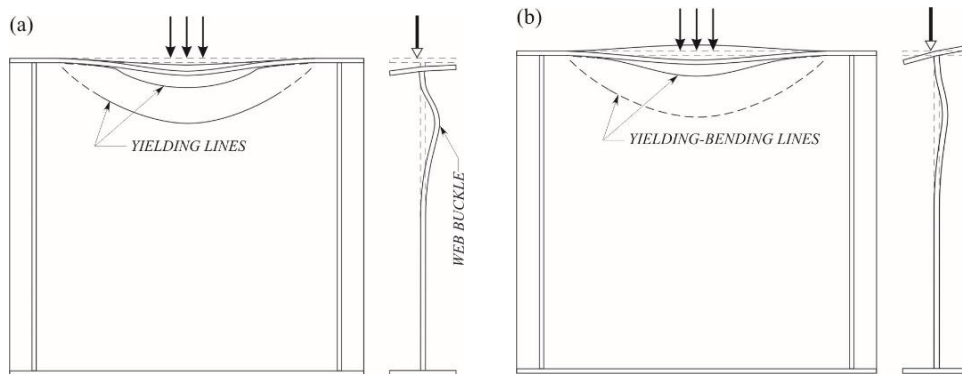


Fig. 5 Mixed collapse mode of eccentrically patch loaded I-girders (M) – variants:
 (a) centric-mixed collapse mode (gentle torsion of flange, centric collapse of web);
 (b) eccentric-mixed collapse mode (pronounced torsion of flange, undefined web collapse)

Based on the experimental data, collapse mode identification criteria summarised in Table 1 have been established. These criteria correlate dimensionless geometry parameters t_f/t_w and $a/t_w = h_w/t_w$ with the dimensionless load eccentricity e/b_f , e/t_f or e/t_w . Such correlations provide high level of reliability in collapse mode identification. Combining (checking) several of these criteria increases the reliability level.

It has to be kept in mind that data from experiments done at the University of Montenegro [26-28] were used for this analysis, i.e. girders dimensions, load eccentricity and load length in range: (0) $5 \text{ mm} \leq e \leq 30 \text{ mm}$, $3 \text{ mm} \leq t_w \leq 10 \text{ mm}$, $3 \text{ mm} \leq t_f \leq 15 \text{ mm}$, $a = h_w = 700 \text{ mm}$, $b_f = 150 \text{ mm}$, $c = 50$ or 150 mm ; and dimensionless geometry parameters in range: (0) $1/30 \leq e/b_f \leq 1/5$, (0) $0.33 \leq e/t_f \leq 8.33$, (0) $0.50 \leq e/t_w \leq 8.33$, $1 \leq t_f/t_w \leq 5$, $10 \leq b_f/t_f \leq 50$, $70 \leq a/t_w = h_w/t_w \leq 233$, $a/h_w = 1$, $c/a = 0.071$ or 0.214 . Hence, these are the limitations of high-level validity area for criteria from Table 1.

Girders fulfilling criteria in dark grey fields of Table 1 have eccentric collapse mode (E), with the reduced ultimate load. Girders fulfilling criteria in light grey fields of Table 1

might have any collapse mode (E, M, C) and these criteria imply that such girders should be carefully analysed each separately, with its specific characteristics, considering several influential parameters and their combinations, as well as paying particular attention to the initial deformation. Girders fulfilling criteria in white (i.e. no highlighted) fields of Table 1 will behave as if there is no load eccentricity (C collapse mode), having same ultimate load as in case of centric patch load.

Primary influential parameter t_f/t_w enables high quality identification of collapse mode in correlation with each one of the three dimensionless eccentricities. However, web slenderness $a/t_w = h_w/t_w$, not encompassing flange thickness t_f , correlated with any of the three eccentricities does not provide comprehensive, exact collapse mode determination.

As a complement to criteria from Table 1, but also in case of its standalone use, ANN modelling proved to be confidential method for collapse mode identification in case of girder geometry when all collapse modes are possible, as illustrated in Figs. 6 and 7. Several networks of various architecture were created and trained, by means of ANN software developed for the needs of research at the University of Montenegro. Two ANN forecast models for collapse mode are chosen for representation herein. Both ANN models displayed at Figs. 6 and 7 have good match with experimental data, particularly considering “pure” eccentric and centric collapse modes (E, C). Tolerable discrepancy may be observed in domain of mixed collapse modes. Trend of ANN models in that domain is completely in accordance with experimental findings. Better fitting of individual points may be achieved by further ANN modelling, which is generally endless activity. Another software or selection of training/verification dataset, as well as fine tuning of ANN models (e.g. different choice of numerals for collapse modes in this specific software etc.) will provide different forecasts. *Note:* In order to apply available ANN software, collapse mode types needed to be assigned numerals and they are chosen in interval [-1, 1], as follows: eccentric collapse mode E = -1; mixed collapse modes $-1 < M < 1$; centric collapse mode C = 1.

Table 1 Criteria for identification of collapse mode in eccentrically patch loaded I-girders

dimensionless load eccentricity	correlated dimensionless parameter	criterion	collapse mode*
e/b_f	h_w/t_w	$h_w/t_w < 1050 \cdot e/b_f + 35$	E
		$h_w/t_w \geq 1050 \cdot e/b_f + 35$	E, M, C
	t_f/t_w	$t_f/t_w < 15 \cdot e/b_f + 0.5$	E
		$15 \cdot e/b_f + 0.5 \leq t_f/t_w \leq 15 \cdot e/b_f + 1.5$	E, M, C
		$t_f/t_w > 15 \cdot e/b_f + 1.5$	C
e/t_f	h_w/t_w	$h_w/t_w \leq 85 \cdot e/t_f + 60$	E
		$85 \cdot e/t_f + 25 \leq h_w/t_w \leq 85 \cdot e/t_f + 105$	M**
	t_f/t_w	$h_w/t_w \geq 85 \cdot e/t_f + 70$	C
		$t_f/t_w < e/t_f + 0.5$	E
		$e/t_f + 0.5 \leq t_f/t_w \leq e/t_f + 1.7$	E, M, C
		$t_f/t_w > e/t_f + 1.7$	C
e/t_w	t_f/t_w	$t_f/t_w < 0.3 \cdot e/t_w + 0.8$	E
		$0.3 \cdot e/t_w + 0.8 \leq t_f/t_w \leq 0.3 \cdot e/t_w + 1.8$	E, M, C
		$t_f/t_w > 0.3 \cdot e/t_w + 1.8$	C

* E = eccentric, M = mixed, C = centric collapse mode

** criterion is not sufficiently precise, detailed analysis of each girder, separately, is necessary

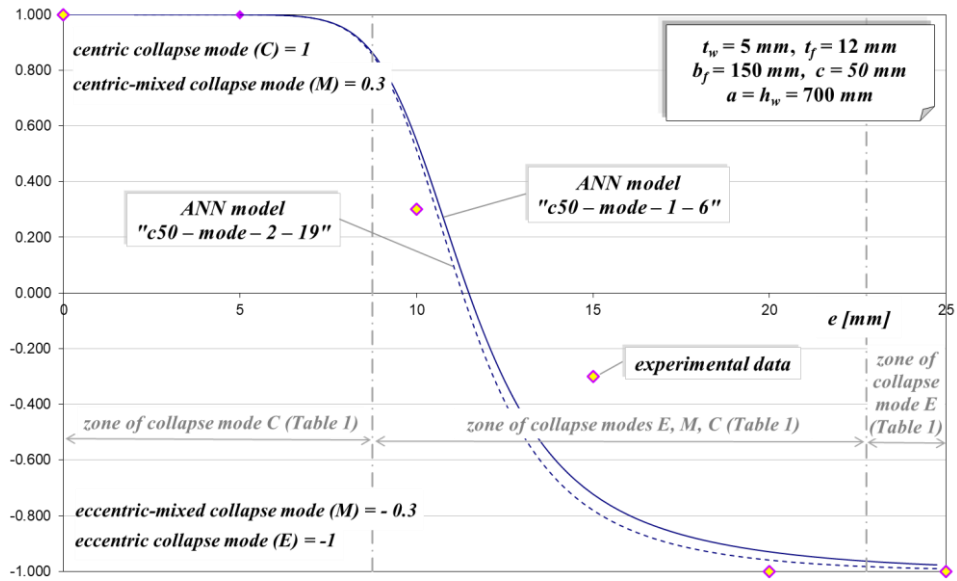


Fig. 6 Illustration of collapse mode identification by means of ANN modelling and according to criteria from Table 1, compared to experimental data, for girders geometry: $t_w = 5 \text{ mm}, t_f = 12 \text{ mm}, a = h_w = 700 \text{ mm}, b_f = 150 \text{ mm}, c = 50 \text{ mm}$

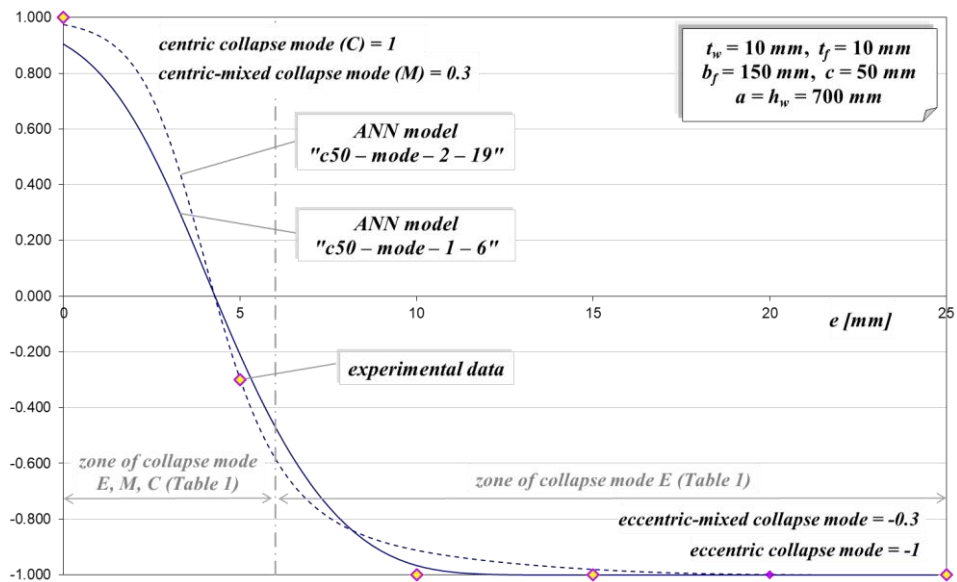


Fig. 7 Illustration of collapse mode identification by means of ANN modelling and according to criteria from Table 1, compared to experimental data, for girders geometry: $t_w = 10 \text{ mm}, t_f = 10 \text{ mm}, a = h_w = 700 \text{ mm}, b_f = 150 \text{ mm}, c = 50 \text{ mm}$

Figs. 6 and 7 exhibit very good match of ANN modelling of collapse mode with criteria from Table 1, not only in outer zones of exclusively centric or eccentric collapse modes (C or E), but also in the middle zone, where all types of collapse mode are possible (C, M, E).

Some girder dimensions or dimensionless parameters, analysed separately, without correlating them with other parameter(s), may be used as a rough identifiers of collapse mode. Girders having thin flange ($t_f \leq 6 \text{ mm}$) or thick web ($t_w \geq 8 \text{ mm}$, e.g. Fig. 7) or low web slenderness ($h_w/t_w < 100$, e.g. Fig. 7) or ratio $t_f/t_w < 2$ (e.g. Fig. 7) are affected even with the lowest eccentricity, as confirmed in Fig. 7. On the other side, girders with the ratio $t_f/t_w > 3$ have centric collapse mode even at the highest load eccentricity. Similarly to these conclusions, drawn from the experimental testing, the accuracy limitations of mechanical model, by Graciano and Uribe-Henao [30], are set up by means of load eccentricity, e , and t_f/t_w ratio: the mechanical model describing eccentric collapse mode should be used when $e \geq 10 \text{ mm}$ and $t_f/t_w \leq 2.5$. It may be concluded that two sets of limits for collapse modes are in a proper agreement, as confirmed in Figs. 6 and 7.

Obviously, apart from the load eccentricity, e , collapse mode depends on both plate thicknesses, t_f and t_w , as well as on their relation, so that parameter t_f/t_w has the key-role in collapse mode determination, regardless of being analysed in co-relation with the other parameters or separately, only by itself.

3. ULTIMATE LOAD OF ECCENTRICALLY PATCH LOADED STEEL I-GIRDERS

From the engineering practice aspect, the most significant characteristic of eccentric and mixed collapse modes is decrease in ultimate load with the increase in load eccentricity. Experiments revealed that the ultimate load decrease of over 40% is possible even in cases of such a small load eccentricity of only 5 mm (i.e. $e/b_f = 1/30$), while larger eccentricity, of 25 mm (i.e. $e/b_f = 1/6$), may decrease ultimate load up to 75%.

FEM modelling, based on non-linear analysis, may provide confident results for ultimate load, but it is not always comfortable to be used by engineers. For common situations in practice, simple calculation procedures are appreciated. Two types of such expressions for ultimate strength of eccentrically patch loaded girders may be found in literature: empirical expressions [28,29], obtained by statistical processing of primarily experimental, but also FEM results, and mathematical expression based on plastic collapse mechanism [30]. ANN modelling may be of great help in determination of ultimate load, whether ANN forecast models are used directly for ultimate load [25], or this tool is coupled with some of previously mentioned methods/expressions, for determination of certain parameters figuring in those expressions for ultimate load.

3.1 Expressions for Ultimate Load

3.1.1 Empirical Procedure – Expression for Reduction Coefficient

Empirical procedure relates the ultimate load of eccentric collapse mode to the ultimate load of centric collapse mode, in girders of same geometry with and without load eccentricity, by introducing reduction coefficient, R , as:

$$R = \frac{\text{ultimate load of eccentrically loaded girder}}{\text{ultimate load of centrally loaded girder}} \quad (1)$$

The ultimate load of centrally loaded girder might be determined by some of numerous expressions proposed in literature, including design norms. Reliable reduction coefficient, R , will then provide ultimate load of eccentrically loaded girder with acceptable accuracy. For the further analysis in this paper, the following expression for reduction coefficient, proposed by Ščepanović et al. [28], will be used:

$$\left. \begin{aligned} R &= m \cdot \left(\frac{e}{b_f}\right)^2 + n \cdot \left(\frac{e}{b_f}\right) + 1.01 \leq 1 \\ m &= -0.864 \cdot \left(\frac{t_f}{t_w}\right)^2 - 14.40 \cdot \left(\frac{t_f}{t_w}\right) + 38.00 \\ n &= -12.30 + 4.22 \cdot \left(\frac{t_f}{t_w}\right) \end{aligned} \right\}. \quad (2)$$

Eq. (2) provides valid results for input in range of data used for its derivation (experimental data reported in [26-28] and FEM data reported in [28]), as follows: $1 \leq t_f/t_w \leq 5$, $(0) 1/30 \leq e/b_f \leq 1/5$, $45 \leq a/t_w \leq 233$, $6.25 \leq b_f/t_f \leq 50$, $1 \leq a/h_w \leq 2$, $0.036 \leq c/a \leq 0.071$ or $c/a = 0.214$.

3.1.2 Expression Based on Mechanical Model of Collapse

Only one mathematical/analytical expression based on plastic collapse mechanism has been proposed so far, by Graciano and Uribe-Henao [30]:

$$\left. \begin{aligned} P_u &= M_f \cdot \left(2\beta\xi + c\xi + \frac{b_f - 2e}{\beta}\right) + M_w \cdot \frac{2\beta + c}{\alpha \cos\theta} \\ M_f &= f_{yf} t_f^2 / 4 & M_w &= f_{yw} t_w^2 / 4 \\ \xi &= b_f / (e(b_f - 2e)) \\ \cos\theta &= \frac{3 f_{yf} \alpha (c + 0.7a)}{8 G b_f t_f} \\ \beta &= \sqrt{\frac{M_f (b_f / 2 - e) \cdot \alpha \cos\theta}{M_w + M_f \xi \cdot \alpha \cos\theta}} \\ \tilde{\alpha} &= 1.9447 t_w \left(\frac{e}{b_f} \cdot \left(\frac{t_w}{t_f}\right)^3\right)^{-0.451} \end{aligned} \right\}, \quad (3)$$

where: M_f and M_w are plastic moments per unit length of yielding line in the flange and web, respectively; f_{yf} and f_{yw} are flange and web yield stresses, respectively; $G = 81000$ MPa is the shear modulus for steel; α , β , θ and ξ are geometrical parameters describing yielding lines and deformed girder geometry in the collapse mechanism. They differ in character, i.e. in method of obtaining. While ξ is used only as a symbol to shorten writing, α , β and θ have clear geometrical meaning explained in [30]. While β and θ are defined analytically, based on mechanical models, by mathematical calculation, α (= distance of the web yielding line from the loaded flange, Fig. 3) may be determined as $\tilde{\alpha}$, using the expression from Eq. (3), obtained by regression analysis, based on the experimental data [30].

To provide accuracy of Eq. (3), Graciano and Uribe-Henao [30] set up following limits: $e \geq 10$ mm and $t_f/t_w \leq 2.5$. These limits and need of more precise definition of Eq. (3) validity area are going to be discussed herein.

3.2 ANN Modelling as Support for Ultimate Load Calculation

In addition to its successful standalone application for direct determination of ultimate load [25], ANN modelling may be used as a very convenient and welcome tool combined with other methods in order to improve them and provide more precise values of ultimate load. Such coupling of ANN modelling with expressions for ultimate load may be characterised as *hybrid modelling*. It is going to be presented herein, at the example of refining Eq. (3) by means of ANN modelling.

Experimental database from 1998 [26], 2001 [27] and 2007 [28], containing 135 test samples, has been used for various ANN training and ANN forecast models creation. Also, comparison of different methods for determination of ultimate load and/or necessary parameters has been done using these test data.

Tables 2 and 3 comprise tested girders geometry data, experimental collapse mode type, α and P_u values obtained by different methods (all calculated and ANN determined P_u values are related to respective experimental values, so to provide easier data comparison):

- experimental position of web yielding lines α_{exp} , (Table 2);
- experimental collapse loads $P_{u,exp}$, (Table 2);
- ultimate loads $P_{u,ANN}$ obtained by ANN forecast models (as $P_{u,ANN}/P_{u,exp}$), (Table 3);
- ultimate loads $P_{u,Eqs(1-2)}$ obtained by Eqs. (1) and (2) when $P_{u,centr} = P_{u,exp}^{(e=0)}$ (as $P_{u,Eqs(1-2)}/P_{u,exp} = R_{Eq(2)}/R_{exp}$), (Table 3);
- $\tilde{\alpha}$ values, obtained by expression from Eq. (3), (Table 2);
- ultimate loads $P_{u,Eq(3)}$ obtained by Eq. (3), including expression for $\tilde{\alpha}$ (as $P_{u,Eq(3)}/P_{u,exp}$), (Table 2);
- ultimate loads $P_{u,Eq(3)-exp}$ obtained by expression for P_u from Eq. (3), but with α_{exp} values (as $P_{u,Eq(3)-exp}/P_{u,exp}$) – experimentally refined Eq. (3), (Table 2);
- α_{ANN} values, obtained by ANN modelling, (Table 2);
- ultimate loads $P_{u,Eq(3)-ANN}$ obtained by expression for P_u from Eq. (3), but with α_{ANN} values (as $P_{u,Eq(3)-ANN}/P_{u,exp}$) – hybrid modelling of P_u , (Table 2).

Complete calculation, as well as creation of ANN models were done with real values of yield stresses f_{yf} and f_{yw} , determined experimentally (Table 3), and $G = 81 \text{ GPa}$.

Table 2 Summary of α values (α_{exp} , $\tilde{\alpha}$, α_{ANN}), experimental collapse loads ($P_{u,exp}$) and ultimate loads determined by original and refined Eq. (3) ($P_{u,Eq(3)}$, $P_{u,Eq(3)-exp}$, $P_{u,Eq(3)-ANN}$), all related to $P_{u,exp}$, for experimental database from 1998, 2001 and 2007 tests [26-28]

No.	girder	t_w	t_f	e	collapse mode	α_{exp}	$P_{u,exp}$	$\tilde{\alpha}$	$\frac{P_{u,Eq(3)}}{P_{u,exp}}$	$\frac{P_{u,Eq(3)-exp}}{P_{u,exp}}$	α_{ANN}	$\frac{P_{u,Eq(3)-ANN}}{P_{u,exp}}$
									[mm]	[kN]		[mm]
1	EB I - 1	3	15	0	C		133					
2	EB I - 2	3	15	5	C		128	238.7	3.10		55.5	3.14
3	EB I - 3	3	15	10	C		127	174.6	2.01		55.4	2.04
4	EB I - 4	3	15	15	C		135	145.4	1.49		55.2	1.52
5	EB I - 5	3	15	20	C		134	127.7	1.28		54.9	1.31
6	EB I - 6	3	15	25	C		124	115.5	1.24		54.6	1.27
7	EB II/III - 1	6	15	0	C		341					
8	EB II/III - 2	6	15	5	C		321	186.9	1.25		53.2	1.30
9	EB II/III - 3	6	15	10	C		313	136.7	0.84		52.9	0.88
10	EB II/III - 4	6	15	15	E	50	282	113.9	0.75	0.80	52.5	0.79
11	EB II/III - 5	6	15	20	E	50	235	100.0	0.78	0.83	52.1	0.83
12	EB II/III - 6	6	15	25	E	55	192	90.4	0.86	0.91	51.6	0.92
13	EB IV - 1	8	15	0	C		401					

12 B. ŠČEPANOVIĆ, S. RUTEŠIĆ, O. MIJUŠKOVIĆ, L.M. GIL-MARTÍN, E. HERNÁNDEZ-MONTES

14	EB IV - 2	8	15	5	C		418	168.8	0.97		52.7	1.03
15	EB IV - 3	8	15	10	E	45	394	123.5	0.68	0.75	52.3	0.73
16	EB IV - 4	8	15	15	E	60	301	102.9	0.72	0.77	51.9	0.79
17	EB IV - 5	8	15	20	E	50	245	90.4	0.78	0.86	51.5	0.85
18	EB IV - 6	8	15	25	E	45	209	81.7	0.84	0.94	51.0	0.91
19	EB V - 1	5	10	0	C		229					
20	EB V - 2	5	10	5	CM		212	115.2	0.97		43.5	1.00
21	EB V - 3	5	10	10	E	40	197	84.2	0.68	0.71	42.8	0.71
22	EB V - 4	5	10	15	E	43	175	70.2	0.62	0.64	42.0	0.64
23	EB V - 5	5	10	20	E	47	153	61.6	0.62	0.63	41.1	0.64
24	EB V - 6	5	10	25	E	50	129	55.7	0.66	0.67	40.2	0.69
25	EB VI - 1	10	10	0	C		720					
26	EB VI - 2	10	10	5	EM		575	90.2	0.39		24.0	0.48
27	EB VI - 3	10	10	10	E	22.5	365	66.0	0.44	0.59	23.3	0.58
28	EB VI - 4	10	10	15	E	22.5	313	54.9	0.45	0.60	22.6	0.60
29	EB VI - 5	10	10	20	E	22.5	275	48.3	0.47	0.63	22.0	0.64
30	EB VI - 6	10	10	25	E	22.5	220	43.6	0.57	0.75	21.5	0.76
31	EB VII - 1	5	12	0	C		230					
32	EB VII - 2	5	12	5	C		225	147.4	1.23		50.1	1.26
33	EB VII - 3	5	12	10	CM		212	107.8	0.85		49.7	0.88
34	EB VII - 4	5	12	15	EM		180	89.8	0.80		49.2	0.83
35	EB VII - 5	5	12	20	E	25	170	78.9	0.73	0.83	48.7	0.76
36	EB VII - 6	5	12	25	E	25	149	71.3	0.75	0.86	48.0	0.78
37	EB VIII - 1	3	3	0	E/EM		79					
38	EB VIII - 2	3	3	5	E	22.5	44	27.0	0.41	0.42	22.5	0.42
39	EB VIII - 3	3	3	10	E	22.5	37	19.8	0.35	0.34	22.0	0.35
40	EB VIII - 4	3	3	15	E	22.5	29	16.5	0.40	0.37	21.5	0.37
41	EB VIII - 5	3	3	20	E	22.5	23	14.5	0.47	0.41	21.1	0.42
42	EB VIII - 6	3	3	25	E	22.5	20	13.1	0.52	0.44	20.7	0.45
43	EB IX - 1	3	6	0	C		95					
44	EB IX - 2	3	6	5	EM		80	69.1	0.86		33.1	0.88
45	EB IX - 3	3	6	10	E	40	69	50.5	0.66	0.67	32.2	0.67
46	EB IX - 4	3	6	15	E	25	57	42.1	0.64	0.67	31.3	0.66
47	EB IX - 5	3	6	20	E	25	47	37.0	0.68	0.71	30.4	0.69
48	EB IX - 6	3	6	25	E	25	39	33.4	0.75	0.78	29.5	0.76
49	EB X - 1	3	9	0	C		102					
50	EB X - 2	3	9	5	C		105	119.6	1.44		25.5	1.48
51	EB X - 3	3	9	10	C		107	87.5	0.91		44.9	0.93
52	EB X - 4	3	9	15	CM		90	72.9	0.86		44.2	0.88
53	EB X - 5	3	9	20	E	50	85	64.0	0.78	0.79	43.4	0.80
54	EB X - 6	3	9	25	E	50	70	57.9	0.85	0.86	42.5	0.87
55	EB XI - 1	3	12	0	C		116					
56	EB XI - 2	3	12	5	C		113	176.5	2.42		53.0	2.44
57	EB XI - 3	3	12	10	C		115	129.1	1.53		52.7	1.55
58	EB XI - 4	3	12	15	C		110	107.5	1.26		52.4	1.28
59	EB XI - 5	3	12	20	CM		105	94.5	1.13		52.1	1.15
60	EB XI - 6	3	12	25	CM		115	85.4	0.92		51.7	0.94
61	EB XII - 1	4	4	0	C/CM		120					
62	EB XII - 2	4	4	5	E	25	70	36.1	0.47	0.49	22.4	0.50
63	EB XII - 3	4	4	10	E	25	50	26.4	0.48	0.48	21.9	0.50
64	EB XII - 4	4	4	15	E	25	45	22.0	0.47	0.45	21.4	0.47
65	EB XII - 5	4	4	20	E	25	40	19.3	0.49	0.45	21.0	0.48
66	EB XII - 6	4	4	25	E	25	35	17.5	0.54	0.48	20.6	0.51
67	EB XIII - 1	4	6	0	C		125					
68	EB XIII - 2	4	6	5	EM		110	62.4	0.64		28.7	0.67
69	EB XIII - 3	4	6	10	E	25	86	45.7	0.55	0.59	27.8	0.58
70	EB XIII - 4	4	6	15	E	25	68	38.0	0.58	0.62	27.0	0.61
71	EB XIII - 5	4	6	20	E	25	50	33.4	0.70	0.74	26.3	0.73
72	EB XIII - 6	4	6	25	E	15	45	30.2	0.72	0.87	25.5	0.75
73	EB XIV - 1	4	8	0	C		140					
74	EB XIV - 2	4	8	5	C		129	92.1	0.99		37.2	1.02
75	EB XIV - 3	4	8	10	C		130	67.4	0.65		36.3	0.67
76	EB XIV - 4	4	8	15	E	50	100	56.1	0.68	0.68	35.3	0.70
77	EB XIV - 5	4	8	20	E	37.5	86	49.3	0.69	0.71	34.3	0.71

78	EB XIV - 6	4	8	25	E	37.5	75	44.6	0.72	0.73	33.3	0.74
79	EB XV - 1	4	10	0	C		155					
80	EB XV - 2	4	10	5	C		148	124.6	1.39		44.8	1.41
81	EB XV - 3	4	10	10	C		140	91.1	0.95		44.2	0.97
82	EB XV - 4	4	10	15	CM		138	75.9	0.77		43.4	0.79
83	EB XV - 5	4	10	20	EM		128	66.7	0.71		42.7	0.74
84	EB XV - 6	4	10	25	EM		115	60.3	0.72		41.8	0.74
85	EB XVI - 1	5	6	0	C		187					
86	EB XVI - 2	5	6	5	E	25	130	57.7	0.56	0.60	27.2	0.59
87	EB XVI - 3	5	6	10	E	25	105	42.2	0.48	0.52	26.5	0.51
88	EB XVI - 4	5	6	15	E	25	74	35.2	0.57	0.62	25.7	0.61
89	EB XVI - 5	5	6	20	E	25	59	30.9	0.66	0.69	25.0	0.69
90	EB XVI - 6	5	6	25	E	25	55	27.9	0.66	0.69	24.3	0.69
91	EB XVII - 1	5	8	0	C		209					
92	EB XVII - 2	5	8	5	CM		200	85.1	0.65		35.5	0.68
93	EB XVII - 3	5	8	10	E	35	145	62.3	0.60	0.63	34.6	0.63
94	EB XVII - 4	5	8	15	E	32	130	51.9	0.54	0.58	33.6	0.57
95	EB XVII - 5	5	8	20	E	28	98	45.6	0.64	0.69	32.6	0.67
96	EB XVII - 6	5	8	25	E	25	83	41.2	0.69	0.76	31.6	0.73
97	EB XVIII - 1	6	6	0	C/CM		208					
98	EB XVIII - 2	6	6	5	E	25	170	54.1	0.44	0.49	23.3	0.50
99	EB XVIII - 3	6	6	10	E	20	130	39.6	0.46	0.58	16.8	0.63
100	EB XVIII - 4	6	6	15	E	15	104	33.0	0.53	0.74	16.7	0.70
101	EB XVIII - 5	6	6	20	E		88	29.0	0.60		16.6	0.78
102	EB XVIII - 6	6	6	25	E		69	26.2	0.75		16.6	0.95
103	EB XIX - 1	6	9	0	C/CM		330					
104	EB XIX - 2	6	9	5	E	20	285	93.6	0.56	0.69	19.6	0.69
105	EB XIX - 3	6	9	10	E	20	217	68.5	0.51	0.67	19.3	0.68
106	EB XIX - 4	6	9	15	E	20	155	57.0	0.61	0.82	19.0	0.84
107	EB XIX - 5	6	9	20	E	20	125	50.1	0.69	0.94	18.7	0.96
108	EB XIX - 6	6	9	25	E		107	45.3	0.76		18.5	1.06
109	EB XX - 1	6	12	0	C		300					
110	EB XX - 2	6	12	5	EM		265	138.2	1.05		46.6	1.09
111	EB XX - 3	6	12	10	E	25	311	101.1	0.60	0.73	26.2	0.73
112	EB XX - 4	6	12	15	E	25	235	84.2	0.66	0.82	25.5	0.82
113	EB XX - 5	6	12	20	E	25	202	74.0	0.68	0.86	24.8	0.86
114	EB XX - 6	6	12	25	E		165	66.9	0.76		24.2	0.99
115	B I/II 5	5	10	0	C		259					
116	EB XXI - 2	5	10	5	C		250	115.2	1.50		43.5	1.54
117	EB XXI - 1	5	10	10	CM		240	84.2	0.95		42.8	0.99
118	B III 1/1	5	10	15	E	75	202	70.2	0.80	0.79	40.7	0.84
119	B III ½	5	10	20	E	70	171	61.6	0.81	0.80	39.8	0.86
120	B III 1/3	5	10	25	E	65	141	55.7	0.90	0.88	38.9	0.95
121	B III ¼	5	10	30	E	60	122	51.3	0.98	0.96	37.9	1.03
122	B I/II 11	10	10	0	C		801					
123	EB XXI - 4	10	10	5	E	22.5	790	90.2	0.51	0.65	24.0	0.64
124	EB XXI - 3	10	10	10	E	50	640	66.0	0.43	0.45	23.3	0.57
125	B III 2/1	10	10	15	E	50	387	54.9	0.55	0.56	25.5	0.73
126	B III 2/2	10	10	20	E	47.5	297	48.3	0.67	0.67	24.9	0.89
127	B III 2/3	10	10	25	E	45	254	43.6	0.75	0.74	24.2	1.00
128	B III 2/4	10	10	30	E	42.5	219	40.2	0.86	0.84	23.6	1.13
129	B I/II 6	5	12	0	C		266					
130	EB XXI - 6	5	12	5	C		255	147.4	1.97		50.1	2.02
131	EB XXI - 5	5	12	10	C		255	107.8	1.19		49.7	1.23
132	B III 3/1	5	12	15	E	85	228	89.8	0.96	0.97	48.4	1.01
133	B III 3/2	5	12	20	E	70	177	78.9	1.06	1.07	47.8	1.12
134	B III 3/3	5	12	25	E	65	162	71.3	1.05	1.06	47.0	1.10
135	B III ¾	5	12	30	E	60	147	65.7	1.08	1.09	46.3	1.13
For all girders: $a = h_w = 700 \text{ mm}$, $b_f = 150 \text{ mm}$							Series B I, B II, B III - 1998 tests [26]					
For samples Nos. 1-114: $c = 50 \text{ mm}$							Series EB I - EB IV - 2001 tests [27]					
For samples Nos. 115-135: $c = 150 \text{ mm}$							Series EB V - EB XXI - 2007 tests [28]					

Table 3 Summary of material properties (f_{yf}, f_{yw}) and ultimate loads determined by Eqs. (1) and (2) and forecasted by ANN models ($P_{u,Eqs(1-2)}, P_{u,ANN}$), both related to $P_{u,exp}$, for experimental database from 1998, 2001 and 2007 tests [26-28]

No.	series	f_{yw} [MPa]	f_{yf} [MPa]	e [mm]							
				0	5	10	15	20	25	30	
1-6	EB I	327.3	268.7	1.00	1.04	1.05	0.99	0.99	1.00	$P_{u,Eqs(1-2)}/P_{u,exp}$	
				1.02	1.01	1.03	0.99	1.00	1.01	$P_{u,ANN}/P_{u,exp}$	
7-12	EB II/III	309.3	268.7	1.00	0.39	0.37	0.38	0.41	0.43	$P_{u,Eqs(1-2)}/P_{u,exp}$	
				0.99	1.01	1.00	1.00	1.01	1.00	$P_{u,ANN}/P_{u,exp}$	
13-18	EB IV	262.4	268.7	1.00	0.84	0.77	0.87	0.93	0.96	$P_{u,Eqs(1-2)}/P_{u,exp}$	
				1.23	1.00	0.92	1.01	1.00	0.93	$P_{u,ANN}/P_{u,exp}$	
19-24	EB V	270.9	309.7	1.00	0.96	0.90	0.89	0.89	0.93	$P_{u,Eqs(1-2)}/P_{u,exp}$	
				1.01	1.00	0.99	1.01	1.01	1.04	$P_{u,ANN}/P_{u,exp}$	
25=30	EB VI	309.7	309.7	1.00	0.96	1.13	0.99	0.88	0.97	$P_{u,Eqs(1-2)}/P_{u,exp}$	
				0.97	1.01	1.18	1.09	1.00	0.99	$P_{u,ANN}/P_{u,exp}$	
31-36	EB VII	270.9	288.8	1.00	0.96	0.93	0.99	0.94	0.93	$P_{u,Eqs(1-2)}/P_{u,exp}$	
				0.99	0.98	1.03	1.09	0.98	0.97	$P_{u,ANN}/P_{u,exp}$	
37-42	EB VIII	274.4	274.4	1.00	1.38	1.22	1.17	1.16	1.16	$P_{u,Eqs(1-2)}/P_{u,exp}$	
				0.91	1.18	1.08	1.17	1.35	1.45	$P_{u,ANN}/P_{u,exp}$	
43-48	EB IX	274.4	287.3	1.00	1.05	1.07	1.14	1.21	1.28	$P_{u,Eqs(1-2)}/P_{u,exp}$	
				1.11	1.10	1.04	1.00	1.04	1.05	$P_{u,ANN}/P_{u,exp}$	
49-54	EB X	274.4	282.0	1.00	0.97	0.93	1.04	0.99	1.03	$P_{u,Eqs(1-2)}/P_{u,exp}$	
				1.08	0.99	0.91	0.98	0.89	0.94	$P_{u,ANN}/P_{u,exp}$	
55-60	EB XI	274.4	288.8	1.00	1.03	1.01	1.05	1.10	0.85	$P_{u,Eqs(1-2)}/P_{u,exp}$	
				0.97	0.96	0.99	1.04	1.05	0.91	$P_{u,ANN}/P_{u,exp}$	
61-66	EB XII	285.0	285.0	1.00	1.31	1.37	1.14	1.01	1.01	$P_{u,Eqs(1-2)}/P_{u,exp}$	
				0.92	1.14	1.20	1.02	0.95	0.97	$P_{u,ANN}/P_{u,exp}$	
67-72	EB XIII	285.0	287.3	1.00	0.94	0.98	1.02	1.18	1.16	$P_{u,Eqs(1-2)}/P_{u,exp}$	
				1.06	0.97	0.99	0.97	1.08	0.98	$P_{u,ANN}/P_{u,exp}$	
73-78	EB XIV	285.0	300.3	1.00	0.96	0.84	0.95	0.97	0.98	$P_{u,Eqs(1-2)}/P_{u,exp}$	
				1.07	1.05	0.96	1.10	1.07	1.07	$P_{u,ANN}/P_{u,exp}$	
79-84	EB XV	285.0	309.7	1.00	0.99	0.97	0.90	0.87	0.84	$P_{u,Eqs(1-2)}/P_{u,exp}$	
				0.99	0.99	1.02	0.99	0.96	0.97	$P_{u,ANN}/P_{u,exp}$	
85-90	EB XVI	270.9	287.3	1.00	1.14	1.09	1.22	1.24	1.17	$P_{u,Eqs(1-2)}/P_{u,exp}$	
				0.92	1.04	0.98	1.07	1.03	0.89	$P_{u,ANN}/P_{u,exp}$	
91-96	EB XVII	270.9	300.3	1.00	0.88	1.00	0.94	1.06	1.11	$P_{u,Eqs(1-2)}/P_{u,exp}$	
				1.01	0.93	1.10	1.05	1.14	1.12	$P_{u,ANN}/P_{u,exp}$	
97-98	EB XVIII	287.3	287.3	1.00	0.94	0.92	0.86	0.80	0.89	$P_{u,Eqs(1-2)}/P_{u,exp}$	
				1.04	0.98	0.99	0.95	0.93	1.01	$P_{u,ANN}/P_{u,exp}$	
103-108	EB XIX	458.3	282.0	1.00	0.96	1.03	1.19	1.24	1.28	$P_{u,Eqs(1-2)}/P_{u,exp}$	
				1.00	0.91	0.94	1.02	1.00	0.97	$P_{u,ANN}/P_{u,exp}$	
109-110	EB XX	287.3	288.8	1.00	1.00	0.75	0.87	0.89	0.96	$P_{u,Eqs(1-2)}/P_{u,exp}$	
				458.3	288.8	1.01	1.05	1.00	1.08	1.01	0.99
115, 118-121	B I/II, III 1	286.5	274.7	1.00	0.92	0.84	0.87	0.90	0.97	$P_{u,Eqs(1-2)}/P_{u,exp}$	
				116-117	EB XXI	270.9	309.7				
122, 125-128	B I/II, III 2	274.7	274.7	1.00	0.78	0.72	0.89	0.91	0.93	$P_{u,Eqs(1-2)}/P_{u,exp}$	
				123-124	EB XXI	309.7	309.7				
129, 132-135	B I/II, III 3	286.5	267.4	1.00	0.98	0.90	0.91	1.04	0.99	$P_{u,Eqs(1-2)}/P_{u,exp}$	
				130-131	EB XXI	270.9	288.8				

Graphical presentation of data from Tables 2 and 3 is given separately for girders with eccentric or mixed collapse mode (E, M – 92 samples, Nos. 10-12, 15-18, 20-24, 26-30, 33-36, 38-42, 44-48, 52-54, 59, 60, 62-66, 68-72, 76-78, 82-84, 86-90, 92-96, 98-102, 104-108, 110-114, 117-121, 123-128, 132-135, Figs. 8a and 9a) and for girders centric collapse mode (C – 43 samples, Nos. 1-9, 13, 14, 19, 25, 31, 32, 37, 43, 49-51, 55-58, 61, 67, 73-75, 79-81, 85, 91, 97, 103, 109, 115, 116, 122, 129-131, Figs. 8b and 9b), having in mind sense(lessness) and/or (in)appropriateness of certain methods implementation, depending on collapse mode type of eccentrically patch loaded girder.

Fig. 8 depicts α values: α_{exp} , $\tilde{\alpha}$ and α_{ANN} . It is obvious that $\tilde{\alpha}$ values are excessively overestimated for the majority of test samples having eccentric or mixed collapse mode (E, M), Fig. 8a. On the other hand, α_{ANN} values are mostly in range of α_{exp} . This is valid for samples with load length $c = 50 \text{ mm}$ (i.e. samples Nos. 1-114(117)). Situation is different for samples with load length $c = 150 \text{ mm}$ (i.e. samples Nos. 114(117)-135). A satisfying agreement of $\tilde{\alpha}$ and α_{exp} may be noted in this zone, while certain discrepancy between α_{ANN} and α_{exp} occurs in these samples.

An acceptable match between $\tilde{\alpha}$ and α_{exp} in girders with $c = 150 \text{ mm}$, Fig. 8a, also stated by Graciano and Uribe-Henao [30], is expected, having in mind that expression for $\tilde{\alpha}$ is fitted to these experimental data (1998 [26] tests data were used in the regression analysis that provided the expression for $\tilde{\alpha}$ [30]). However, strong disagreement of $\tilde{\alpha}$ values with experimental data for $c = 50 \text{ mm}$ (2001 [27] and 2007 [28] tests), indicates that conditions for application of Eq. (3) should be revised. This mismatch is also expected and easily explainable. Experimental samples from 1998 [26], 2001 [27] and 2007 [28] have same dimensions $a = h_w = 700 \text{ mm}$, $b_f = 150 \text{ mm}$, but different plate thicknesses t_f and t_w , as well as their ratios, which immensely influence girder behaviour, so that three experimental campaigns complement each other in constituting comprehensive database. Considering this simultaneously with the fact of difference in load length, it is clear that the expression for $\tilde{\alpha}$ in Eq. (3) may not be assumed as universal and should be applied only for girders with geometry in range of data used for the regression analysis.

Although parameter α from Eq. (3) does not have (the same) realistic meaning in girders with centric collapse mode (C), i.e. Eq. (3) is not intended for girders with centric collapse mode, illustration Fig. 8b is kept herein, not only to display significant difference between $\tilde{\alpha}$ and α_{ANN} values, but also to point out non-realistically high values of $\tilde{\alpha}$. Actually, several samples in Fig. 8b have parameters e and t_f/t_w at the very border of domain suitable for use of Eq. (3), according to Graciano and Uribe-Henao [30]. Majority of samples from Fig. 8b confirm that Eq. (3) does not provide reliable results for girders with $e < 10 \text{ mm}$ or $t_f/t_w > 2.5$, in addition to the fact that it should not be applied for these girders at all, because they have completely different collapse mechanism.

Consequently, it may be concluded that complete set of Eq. (3) may provide valid results for input in the following range (i.e. range of experimental data reported by Lučić [26], which were used for statistical data procession during Eq. (3) derivation [30]): $1 \leq t_f/t_w \leq 2.4$, $1/10 \leq e/b_f \leq 1/5$, $70 \leq a/t_w \leq 140$, $12.5 \leq b_f/t_f \leq 15$, $a/h_w = 1$, $c/a = 0.214$. Furthermore, Eq. (3), describing eccentric collapse mechanism, should be applied only in girders with eccentric collapse mode, regardless of the existence and level of load eccentricity, and this is, actually, the first precondition for application of Eq. (3).

These constraints are more demanding and more comprehensive than those set up by Graciano and Uribe-Henao [30] ($e/b_f \geq 1/15$, in the context of available experimental data, and $t_f/t_w \leq 2.5$), which are close to, but do not completely fit within newly proposed

conditions and do not cover all influential parameters. Hence, newly proposed constraints (in the previous paragraph) will provide higher reliability of Eq. (3) results.

Discrepancy between α_{ANN} and α_{exp} in samples Nos. 114(117)-135, Fig. 8a, is easily explained by the fact that ANN for α_{ANN} models were trained on experimental data in which $c = 50 \text{ mm}$ prevailed. Hence, those models may not provide perfect forecast for input with $c = 150 \text{ mm}$.

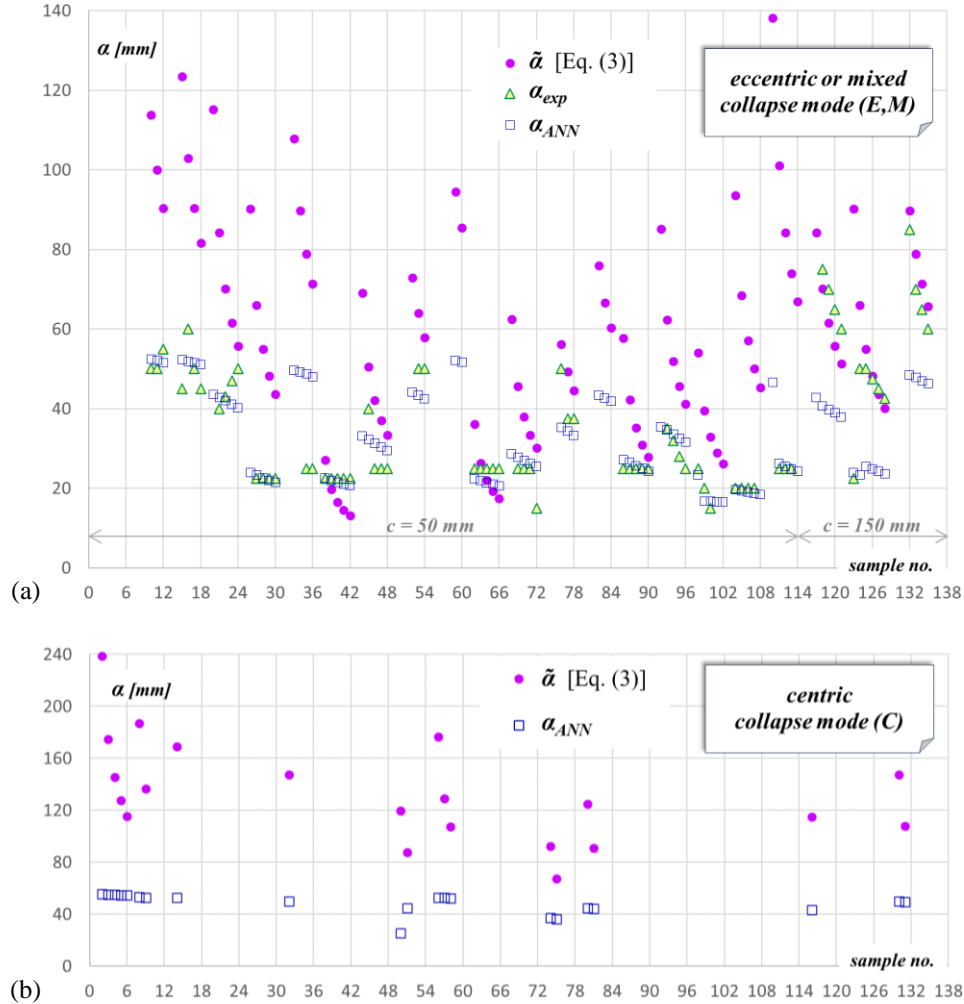


Fig. 8 α values in girders with: (a) eccentric or mixed collapse mode (E, M); (b) centric collapse mode (C)

In Fig. 9, P_u values are compared: experimental values $P_{u,exp}$, values $P_{u,Eq(3)}$ obtained by original Eq. (3), and values $P_{u,Eq(3)-exp}$ and $P_{u,Eq(3)-ANN}$ obtained by refined Eq. (3). Refinement of Eq. (3) is achieved by using α_{exp} or α_{ANN} instead of $\tilde{\alpha}$.

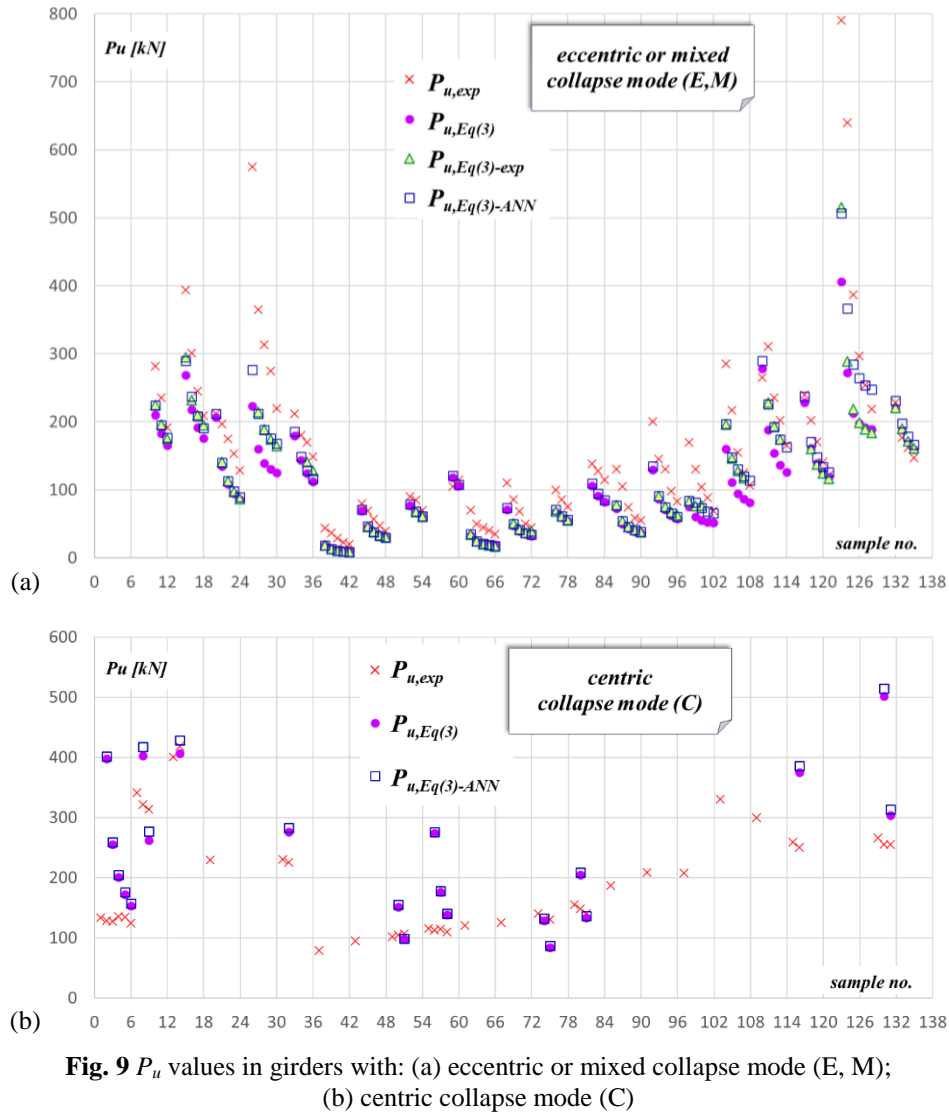


Fig. 9 P_u values in girders with: (a) eccentric or mixed collapse mode (E, M); (b) centric collapse mode (C)

It is clearly noticeable that almost all values of ultimate load obtained by Eq. (3), in its original as well as refined form, are immensely underestimated in girders with eccentric or mixed collapse mode (E, M), Fig. 9a. Calculated values ($P_{u,Eq(3)}$, $P_{u,Eq(3)-exp}$ and $P_{u,Eq(3)-ANN}$) are in average around 71% of experimental values ($P_{u,exp}$), while some of them are as low as only 34% $P_{u,exp}$ (Table 4, middle segment). Both percentages are too low and may not recommend application of Eq. (3) in the whole range of available experimental data. If only samples with load length $c = 50$ mm are analysed (i.e. samples Nos. 1-114(117), with E or M collapse mode), level of underestimation is slightly worse: calculated ultimate loads are in average around 68% $P_{u,exp}$, while minimal calculated value remains 34% $P_{u,exp}$. Concerning only samples with load length $c = 150$ mm (i.e. samples Nos. 114(117)-135,

with E or M collapse mode), both percentages of underestimation are more favourable, i.e. underestimation is less emphasized: calculated values of ultimate loads are in average around 86% $P_{u,exp}$, while minimal calculated value is 48% $P_{u,exp}$. Certain differentiation of these percentages, for $c = 150 \text{ mm}$, in comparison to those reported by Graciano and Uribe-Henao [30] are generally due to differences in yield stresses f_{yf} and f_{yw} (real values are used herein, while Graciano and Uribe-Henao [30] used nominal values), but may also be due to the fact that more samples from this category are analysed herein (15 samples) than by Graciano and Uribe-Henao [30] (12 samples).

Values $P_{u,Eq(3)-ANN}$ are closest to $P_{u,exp}$. In average, they are 75% $P_{u,exp}$ for the whole dataset from Fig. 9a (Table 4, middle segment), 71% $P_{u,exp}$ for $c = 50 \text{ mm}$ and even 93% $P_{u,exp}$ for $c = 150 \text{ mm}$. This is significantly better match than for $P_{u,Eq(3)}$ values, obtained by original Eq. (3), which are the most distant from $P_{u,exp}$: in average 68% $P_{u,exp}$ for the whole dataset from Fig. 9a (Table 4, middle segment), 65% $P_{u,exp}$ for $c = 50 \text{ mm}$ and 82% $P_{u,exp}$ for $c = 150 \text{ mm}$. The beneficial difference of even 11% ($c = 150 \text{ mm}$) speaks in favour of Eq. (3) refinement, achieved by its coupling with ANN α modelling, Fig. 10.

92 samples, with eccentric or mixed collapse mode, are presented in Fig. 9a. Only two of them have ratio $t_f/t_w > 2.5$ and other twelve have load eccentricity $e < 10 \text{ mm}$. Hence, even 85% (78/92) of samples satisfy preconditions for Eq. (3) defined by Graciano and Uribe-Henao [30]. Still, results of Eq. (3) are not appropriate for engineering practice. However, only 29% (27/92) of samples satisfy more realistic (and stricter) preconditions for Eq. (3), suggested herein. This is the main reason for described unacceptable disagreement of original Eq. (3) and experimental results. Thorough analysis of data from Table 2 reveals that exactly these 27 samples (15 samples with $c = 50 \text{ mm}$, Nos: 22-24, 28-30, 34-36, 106-108, 112-114; 12 samples with $c = 150 \text{ mm}$, Nos: 118-121, 125-128, 132-135, that were used for the derivation of Eq. (3)) have the best match of calculated and experimental values of ultimate load, with average calculated value of 81% $P_{u,exp}$ (Table 4, lower segment), i.e. for 10% better than for the whole dataset from Fig. 9a (Table 4, middle segment). Again values $P_{u,Eq(3)-ANN}$ have smallest deviation from $P_{u,exp}$. In average, they are 88% $P_{u,exp}$ (Table 4, lower segment), i.e. for 13% better than for the whole dataset from Fig. 9a (Table 4, middle segment). Statistics enhancement is well pictured in Fig. 11. When samples with different load length are considered separately, results are also significantly better, for both categories. As assumed, samples with $c = 150 \text{ mm}$ have the best match of refined/hybrid calculated and experimental results: in average $P_{u,Eq(3)-ANN} = 98\% P_{u,exp}$.

Obvious shortage of Eq. (3), i.e. its expression for $\tilde{\alpha}$, may be overcome by ANN modelling of α . With α_{ANN} values, instead of $\tilde{\alpha}$, P_u values are remarkably more precise.

Although calculated P_u values (by any version of Eq. (3)) might not be valid ultimate load of eccentrically loaded girders with centric collapse mode (no ultimate load reduction due to load eccentricity, therefore no need and no sense to calculate ultimate load by Eq. (3) or any other procedure related to eccentric load mode), Fig. 9b is displayed herein. It is interesting that, unlike the case of eccentric or mixed collapse mode from Fig. 9a, these “calculated ultimate loads” in Fig. 9b are mostly overestimated, significantly higher than $P_{u,exp}$, which confirms senselessness of these data. Again, even if it is not known that these samples have centric collapse mode, they are almost all out of validity domain of Eq. (3), according to Graciano and Uribe-Henao [30], so that use of Eq. (3) would be inadequate. However, it should be pointed out that Fig. 9b has neither practical purpose nor meaning, primarily because these samples have centric collapse mode, which is not described by Eq. (3), regardless of the boundaries for load eccentricity and girder geometry.

3.3 Comparison of Methods for Ultimate Load Determination

Based on summaries from Tables 2 and 3, general comparison of following methods and procedures for ultimate load determination has been presented:

- empirical procedure, defined by Eqs. (1) and (2) - $P_{u,Eqs(1-2)}$;
- mechanical model, mathematically defined by Eq. (3) in its original form - $P_{u,Eq(3)}$;
- mechanical model coupled with experimental data α_{exp} , i.e. experimentally refined Eq. (3) - $P_{u,Eq(3)-exp}$;
- mechanical model coupled with ANN modelling data α_{ANN} , i.e. ANN refined Eq. (3) (hybrid model) - $P_{u,Eq(3)-ANN}$; and
- ANN forecast model - $P_{u,ANN}$.

For the sake of comparison simplicity, all calculated (by Eqs. (1-3)) and forecasted (by ANN model) values of ultimate load ($P_{u,calc}$) are related to respective experimental collapse loads ($P_{u,exp}$). Statistical parameters (max, min and mean value, standard deviation and coefficient of variation) for ratios $P_{u,calc}/P_{u,exp}$ are determined and summarised in Table 4. Statistics has been done initially for the complete database (135 samples – upper segment of Table 4), then only for samples with eccentric or mixed collapse mode (92 samples – middle segment of Table 4), and finally only for samples with eccentric or mixed collapse mode, satisfying preconditions for applying Eq. (3), as suggested in Chapter 3.2 (27 samples – lower segment of Table 4). Graphical presentation is enclosed for later two cases, Figs. 10 and 11.

Table 4 Statistics parameters for five procedures of ultimate load determination

		$\frac{P_{u,Eqs(1-2)}}{P_{u,exp}}$	$\frac{P_{u,Eq(3)}}{P_{u,exp}}$	$\frac{P_{u,Eq(3)-exp}}{P_{u,exp}}$	$\frac{P_{u,Eq(3)-ANN}}{P_{u,exp}}$	$\frac{P_{u,ANN}}{P_{u,exp}}$
ALL GIRDER (135 SAMPLES)	Max	1.38 [#]	3.10	calc. only for girders with ecc. and mixed collapse mode	3.14	1.45
	Min	0.37	0.35		0.35	0.89
	mean value	0.98	0.82		0.88	1.02
	stand. dev. (S)	0.16	0.40		0.40	0.08*
	coeff. of var. (V)	0.17	0.49		0.45	0.08*
ECCENTRIC OR MIXED COLLAPSE MODE – E, M (92 SAMPLES)	Max	1.38 [#]	1.13	1.09	1.15	1.45
	Min	0.38	0.35	0.34	0.35	0.89
	mean value	0.99	0.68	0.70	0.75	1.03
	stand. dev. (S)	0.18	0.17	0.17	0.19	0.09*
VALIDITY DOMAIN FOR Eq. (3), CHAPTER 3.2 (27 SAMPLES)	Max	1.28	1.08	1.09	1.13	1.09
	Min	0.87	0.45	0.56	0.60	0.97
	mean value	0.97	0.75	0.81	0.88	1.02
	stand. dev. (S)	0.11	0.17	0.15	0.16	0.04
	coeff. of var. (V)	0.11	0.22	0.18	0.18	0.04

Although displayed herein, data from dark grey fields in Table 4 should be exempted from further discussion, since they include ultimate loads obtained by Eq. (3) for girders for which this method is not intended – girders with centric collapse mode. Mean values are above 0.80 (much better than in the middle segment of Table 4), but these are fake information, as a consequence of improper use of Eq. (3), and it should be recognised.

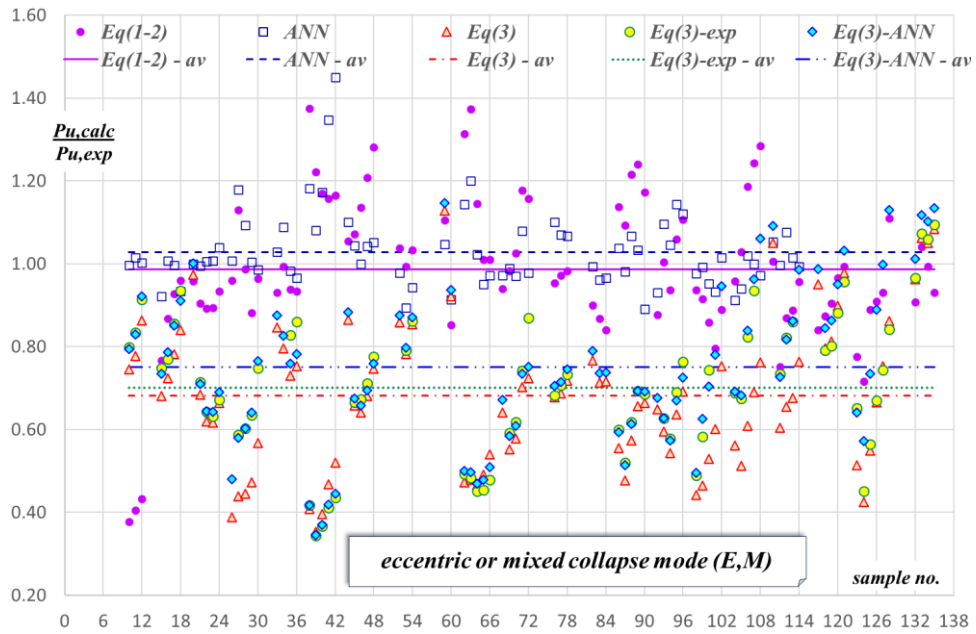


Fig. 10 Ratios of calculated and experimental ultimate load ($P_{u,calc}/P_{u,exp}$) for girders with eccentric or mixed collapse mode (E, M) – set of 92 samples

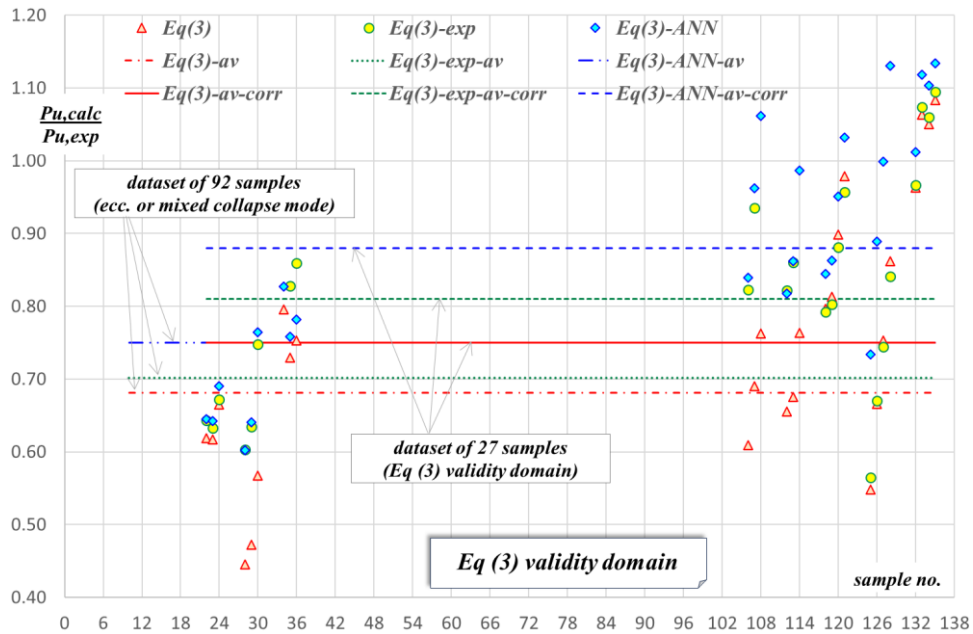


Fig. 11 Ratios of calculated and experimental ultimate load ($P_{u,calc}/P_{u,exp}$) in domain of Eq. (3) validity – set of 27 samples

Statistical parameters of ultimate load obtained by empirical procedure ($P_{u,Eq(1-2)}$) or forecasted by ANN models ($P_{u,ANN}$) do not depend on whether girders with centric collapse mode are included in sample set or not – statistical values are same for set of 135 samples, having various collapse modes (upper segment of Table 4), and for set of 92 samples with eccentric or mixed collapse mode only (middle segment of Table 4). This is due to the fact that both methods are derived from the complete experimental database (135 samples), by statistical “best fitting” techniques. Mean values of both methods are very close to 1, i.e. almost perfect (**bolded numbers** in Table 4; Fig. 10). Somewhat lower standard deviation and coefficient of variation may bring certain advantage to ANN modelling (* marked numbers in Table 4), judging only by statistics. In reality, the fact that empirical procedure approximates experimental values from the safe side (Fig. 10), also having lower max unsafe discrepancy (# marked numbers in Table 4), stands in favour of this method.

Regarding the variants of Eq. (3), its underestimation of ultimate load (*italic underlined numbers* in Table 4) is not tolerable in engineering practice, despite its evident refinement by coupling with ANN modelling (**bold italic underlined number** in Table 4). This method is on the safe side (Figs. 10 and 11), but not simultaneously economical. Statistical parameters for Eq. (3) variants are notably enhanced when it is applied in a real domain of its validity (light grey fields, lower segment of Table 4; Fig. 11). However, even in this narrow domain, i.e. on dataset of only 27 samples, other methods (empirical procedure with reduction coefficient and ANN modelling) provide better statistics and are more favourable, which implies necessity of further revision of Eq. (3), considering complete existing experimental database, exactly as Graciano and Uribe-Henao [30] concluded.

4. CONCLUSION

ANN modelling proved to be valuable in the analysis of eccentrically patch loaded steel I-girders. Well-structured and properly trained artificial neural networks provide reliable forecast models for different needs. They may be used as a self-contained tool for resolving both key-issues: identification of collapse mode type and determination of collapse load. In addition, ANN forecasting may be successfully combined with other methods, in order to complement and/or to refine them, by providing confident determination of certain parameters needed for the other method. Such procedure is denoted as hybrid modelling.

Regarding collapse mode identification, whether used standalone or complemented with empirical criteria, ANN forecast models have very good results. As concerns ultimate load determination, pure ANN modelling provides nearly perfect results, regardless of collapse mode type, which positions this method in top-two procedures for ultimate load. This is of particular importance when girder geometry enables any (or more) collapse mode(s). Applying ANN modelling within mathematical model, as its support to determine specific influential parameter necessary for ultimate load calculation, is highly beneficial, fixes insufficiencies and significantly contributes to the enhancement mechanical model.

Although coupling with ANN modelling considerably improved mechanical model for ultimate load and new, more demanding constraints of its validity are proposed, further revision of mechanical model should be done, based on all available experimental data.

Having in mind that options for improvement of ANN models could hardly be exhausted, future investigation will reveal new advantages and benefits, as well as new fields of use of this AI technique in studying eccentric patch loading in steel I-girders.

REFERENCES

1. Navarro-Manso, A., Del Coz Díaz, J.J., Alonso-Martínez, M., Castro-Fresno, D., Alvarez Rabanal, F.P., 2015, *Patch loading in slender and high depth steel panels: FEM-DOE analyses and bridge launching application*, Engineering Structures, 83, pp. 74-85.
2. Chacón, R., Zorrilla, R., 2015, *Structural health monitoring in incrementally launched steel bridges: Patch loading phenomena modeling*, Automation in Construction, 58, pp. 60-73.
3. Omidali, M., Khedmati, M.R., 2018, *Reliability-based design of stiffened plates in ship structures subject to wheel patch loading*, Thin-Walled Structures, 127, pp. 416-424.
4. Tetougueni, C.D., Maiorana, E., Zampieri, P., Pellegrino, C., 2019, *Plate girders behaviour under in-plane loading: A review*, Engineering Failure Analysis, 95, pp. 332-358.
5. Graciano, C., 2015, *Patch loading resistance of longitudinally stiffened girders – A systematic review*, Thin-Walled Structures, 95, pp. 1-6.
6. Kövesdi, B., 2018, *Patch loading resistance of slender plate girders with longitudinal stiffeners*, Journal of Constructional Steel Research, 140, pp. 237-246.
7. Chacon, R., Herrera, J., Fargier-Gabaldon, L., 2017, *Improved design of transversally stiffened steel plate girders subjected to patch loading*, Engineering Structures, 150, pp. 774-785.
8. Chacon, R., Mirambell, E., Real, E., 2019, *Transversally and longitudinally stiffened steel plate girders subjected to patch loading*, Thin-Walled Structures, 138, pp. 361-372.
9. Arabzadeh, A., Varmazyari, M., 2009, *Strength of I-girders with Delta stiffeners subjected to eccentric patch loading*, Journal of Constructional Steel Research, 65(6), pp. 1385-1391.
10. Casanova, E., Graciano, C., Chacón, R., 2022, *Patch loading resistance of steel plate girders stiffened with triangular cell flanges*, Structures, 38, pp. 993-1004.
11. Inaam, Q., Upadhyay, A., 2020, *Behavior of corrugated steel I-girder webs subjected to patch loading: Parametric study*, Journal of Constructional Steel Research, 165, 105896.
12. Maiorana, E., Poh'sié, G.H., Emechebe, C.C., 2023, *Non-linear Analysis of Corrugated Plate Girders Under Patch Loading*, International Journal of Steel Structures, 23, pp. 758-766.
13. Chacon, R., Mirambell, E., Real, E., 2009, *Influence of designer-assumed initial conditions on the numerical modelling of steel plate girders subjected to patch loading*, Thin-Walled Structures, 47(4), pp. 391-402.
14. Rogač, M., Aleksić, S., Lučić, D., 2020, *Influence of patch load length on resistance of I-girders. Part-I: Experimental research*, Journal of Constructional Steel Research, 175, 106369.
15. Ceranic, A., Bendic, M., Kovacevic, S., Salatic, R., Markovic, N., 2022, *Influence of patch load length on strengthening effect in steel plate girders*, Journal of Constructional Steel Research, 195, 107348.
16. Kövesdi, B., Alcaine, J., Dunai, L., Mirambell, E., Braun, B., Kuhlmann, U., 2014, *Interaction behaviour of steel I-girders Part I: Longitudinally unstiffened girders*, Journal of Constructional Steel Research, 103, pp. 327-343.
17. Chacón, R., Bock, M., Real, E., 2011, *Longitudinally stiffened hybrid steel plate girders subjected to patch loading*, Journal of Constructional Steel Research, 67(9), pp. 1310-1324.
18. Kurtoglu, A.E., Casanova, E., Graciano, C., 2022, *Artificial intelligence-based modeling of extruded aluminum beams subjected to patch loading*, Thin-Walled Structures, 179, 109673.
19. Graciano, C., Loáiza, N., Casanova, E., 2019, *Resistance of slender austenitic stainless steel I-girders subjected to patch loading*, Structures, 20, pp. 924-934.
20. Luo, Z., Shi, Y., Xue, X., Gao, T., Li, H., Xu, J., 2023, *High-strength steel plate girders under patch loading: Numerical analysis and design recommendations*, Structures, 57, 105108.
21. Luo, Z., Shi, Y., Xue, X., Zhou, X., Yao, X., 2023, *Nonlinear patch resistance performance of hybrid titanium-clad bimetallic steel plate girder with web opening*, Journal of Building Engineering, 65, 105703.
22. Xue, X., Shi, Y., Luo, Z., Yao, B., 2023, *Patch-loading resistance performance of stainless-clad bimetallic steel plate girders: Numerical investigations and design methods*, Thin-Walled Structures, 190, 110964.
23. Shi, Y., Luo, Z., Xue, X., Ma, Q., 2024, *Numerical Investigation and Design Suggestion on Patch-Loading Strength of Q690 High-Strength Steel Plate Girders at Elevated Temperature*, Fire Technology, 60, pp. 545-577.
24. CEN, 2006, *EN 1993-1-5:2006, Eurocode 3: Design of steel structures - Part 1-5: General rules - Plated structural elements*
25. Šćepanović, B., Knežević, M., Lučić, D., 2014, *Methods for determination of ultimate load of eccentrically patch loaded steel I-girders*, Informes de la Construcción, 66(EXTRA 1), m018.
26. Lučić, D., 2003, *Experimental research on I-girders subjected to eccentric patch loading*, Journal of Constructional Steel Research, 59(9), pp. 1147-1157.

27. Lučić, D., Šćepanović, B., 2004, *Experimental investigation on locally pressed I-beams subjected to eccentric patch loading*, Journal of Constructional Steel Research, 60(3-5), pp. 525-534.
28. Šćepanović, B., Gil-Martín, L.M., Hernández Montes, E., Aschheim, M., Lučić, D., 2009, *Ultimate strength of I-girders under eccentric patch loading: Derivation of a new strength reduction coefficient*, Engineering Structures, 31(7), pp. 1403-1413.
29. Gil Martín, L.M., Šćepanović, B., Hernández-Montes, E., Aschheim, M., Lučić, D., 2010, *Eccentrically patch loaded steel I-girders: influence of patch length on ultimate strength*. Journal of Constructional Steel Research, 66(5), pp. 716-722.
30. Graciano, C., Uribe-Henao, A.F., 2014, *Strength of steel I-girders subjected to eccentric patch loading*, Engineering Structures, 79, pp. 401-406.
31. Salehi, H., Burgueño, R., 2018, *Emerging artificial intelligence methods in structural engineering*, Engineering Structures, 171, pp. 170-189.
32. Sun, H., Burton, H.V., Huang, H., 2021, *Machine learning applications for building structural design and performance assessment: State-of-the-art review*, Journal of Building Engineering, 33, 101816.
33. Wang, C., Song, L.H., Yuan, Z., Fan, J.S., 2023, *State-of-the-art AI-based computational analysis in civil engineering*, Journal of Industrial Information Integration, 33, 100470.
34. Tapeh, A., Naser, M.Z., 2023, *Artificial intelligence, machine learning, and deep learning in structural engineering: A scientometrics review of trends and best practices*, Archives of Computational Methods in Engineering, 30, pp. 115-159.
35. Chojaczyk, A.A., Teixeira, A.P., Neves, L.C., Cardoso, J.B., Guedes Soares, C., 2015, *Review and application of Artificial Neural Networks models in reliability analysis of steel structures*, Structural Safety, 52(A), pp. 78-89.
36. Markovic, M., Radivojevic, N., Andrejevic Stosovic, M., Markovic Brankovic, J., Zivkovic, S., 2022, *High Embankment Dam Stability Analysis Using Artificial Neural Networks*, Tehnicki vjesnik-Technical Gazette, 29(5), pp. 1733-1740.
37. Zarezadeh, A., Shishesaz, M.R., Ravanavard, M., Ghobadi, M., Zareipour, F., Mahdavian, M., 2023, *Electrochemical and Mechanical Properties of Ni/g-C₃N₄ Nanocomposite Coatings with Enhanced Corrosion Protective Properties: A Case Study for Modeling the Corrosion Resistance by ANN and ANFIS Models*, Journal of Applied and Computational Mechanics, 9(3), pp. 590-606.
38. Mai, S.H., Tran, V.-L., Nguyen, D.-D., Nguyen, V.T., Thai, D.-K., 2022, *Patch loading resistance prediction of steel plate girders using a deep artificial neural network and an interior-point algorithm*, Steel and Composite Structures, 45(2), pp. 159-173.
39. Kumar, S.A., Sofi, F.A., Bhat, J.A., 2023, *Estimation of patch-loading resistance of steel girders with unequal trapezoidal web-corrugation folds using nonlinear FE models and artificial neural networks*, Structures, 48, pp. 1651-1669.